Oscillating bound states for a giant atom

Downloaded from: https://research.chalmers.se, 2025-12-04 23:21 UTC

Citation for the original published paper (version of record):
Guo, L., Frisk Kockum, A., Marquardt, F. et al (2020). Oscillating bound states for a giant atom. Physical Review Research, 2(4). http://dx.doi.org/10.1103/PhysRevResearch.2.043014

N.B. When citing this work, cite the original published paper.

research.chalmers.se offers the possibility of retrieving research publications produced at Chalmers University of Technology. It covers all kind of research output: articles, dissertations, conference papers, reports etc. since 2004. research.chalmers.se is administrated and maintained by Chalmers Library

(article starts on next page)

Oscillating bound states for a giant atom

Lingzhen Guo,[1] Anton Frisk Kockum,[2] Florian Marquardt,[1,3] and Göran Johansson[2]
[1]*Max Planck Institute for the Science of Light, Staudtstraße 2, 91058 Erlangen, Germany*
[2]*Department of Microtechnology and Nanoscience (MC2), Chalmers University of Technology, SE-41296 Göteborg, Sweden*
[3]*Physics Department, University of Erlangen-Nuremberg, Staudtstraße 5, 91058 Erlangen, Germany*

(Received 22 December 2019; accepted 9 September 2020; published 2 October 2020)

We investigate the relaxation dynamics of a single artificial atom interacting, via multiple coupling points, with a continuum of bosonic modes (photons or phonons) in a one-dimensional waveguide. In the non-Markovian regime, where the traveling time of a photon or phonon between the coupling points is sufficiently large compared to the inverse of the bare relaxation rate of the atom, we find that a boson can be trapped and form a stable bound state. As a key discovery, we further find that a persistently oscillating bound state can appear inside the continuous spectrum of the waveguide if the number of coupling points is more than two since such a setup enables multiple bound modes to coexist. This opens up prospects for storing and manipulating quantum information in larger Hilbert spaces than available in previously known bound states.

DOI: 10.1103/PhysRevResearch.2.043014

I. INTRODUCTION

The study of interaction between light and matter is one of the core topics in modern physics [1]. In such studies, the wavelength of the light is usually large compared to the size of the (artificial) atoms constituting the matter [2–7]. Indeed, the traditional framework of quantum optics is based on pointlike atoms [8] and neglects the time it takes for light to pass a single atom. Recently, following significant technological advances for superconducting circuits [7,9–11], "giant" artificial atoms [12] (transmon qubits [13]) have been designed to interact with surface acoustic waves (SAWs) via multiple coupling points in a waveguide [14–16] (or resonator [17–23]) as sketched in Fig. 1 (left inset). Such a giant-atom structure can also be realized in a more conventional circuit-quantum-electrodynamics (circuit-QED) experiment by coupling a single Xmon [24], a version of the transmon, to a meandering coplanar waveguide (CPW) as sketched in Fig. 1 (right inset) [25–27]. Since the distance between coupling points can be (much) longer than the characteristic wavelength of the bath, it is necessary to consider the phase difference between these coupling points. Striking effects have been found as a consequence of this, e.g., frequency-dependent relaxation rate and Lamb shift of a giant atom [25–27], and decoherence-free interaction between multiple giant atoms [26,28]. The giant-atom scheme has recently been extended to higher dimensions with cold atoms [29] and constitutes an exciting new paradigm in quantum optics [10,12,29], where much remains to explore.

Spurred by the growing interest in quantum information science, there have been many investigations of non-Markovian open quantum systems, e.g., single atom(s) in front of a mirror [30–34] or distant atoms coupled locally to the same environment [35–43]. The physical origin of the non-Markovianity is typically the coupling to a structured bath causing information backflow from the environment [44–46]. These systems can exhibit nonexponential relaxation [47,48] and bound states [34,49–60], which can be harnessed for quantum simulations [61,62]. Here, we realize non-Markovianity in a single giant atom by engineering the time delays between coupling points to be comparable to the relaxation time [63,64]. For such a non-Markovian giant atom with *two* coupling points, it has been predicted [63], and recently observed in experiment [16], that the spontaneous decay is polynomial instead of exponential.

In this work, we investigate the relaxation dynamics of a single giant atom interacting with a one-dimensional (1D) bosonic bath (e.g., an open waveguide for phonons or photons) through *multiple* coupling points. Our main result is that *three or more* coupling points enable the creation of *persistently oscillating bound states*, a phenomenon which, to the best of our knowledge, is unique to giant atoms. We envision that this phenomenon could be used for storing and manipulating quantum information in larger Hilbert spaces, and that it could be viewed as a minimalistic implementation of cavity QED with the atom forming its own cavity.

II. MODEL HAMILTONIAN

We consider a two-level atom interacting with an open 1D waveguide at N coupling points (Fig. 1 illustrates the case $N = 3$). As illustrated by the two insets in Fig. 1, this

Published by the American Physical Society under the terms of the Creative Commons Attribution 4.0 International license. Further distribution of this work must maintain attribution to the author(s) and the published article's title, journal citation, and DOI. Open access publication funded by the Max Planck Society.

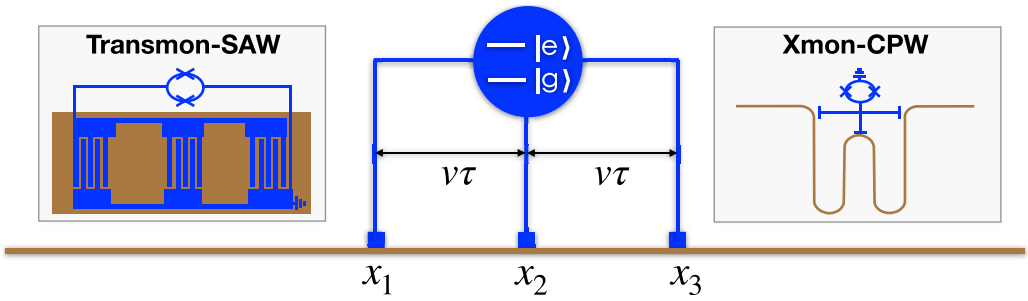

FIG. 1. Sketch and experimental setups for giant atoms. An atom (blue) couples to a waveguide (brown) at multiple points x_j, which are spaced far apart. Left: a transmon qubit coupled to a SAW waveguide via multiple interdigital transducers. Right: an Xmon qubit coupled capacitively to a meandering microwave CPW at multiple points.

system can be implemented in at least two different experimental schemes: a transmon qubit with multiple interdigital transducers (IDTs) coupled to SAWs through piezoelectric effects [14–17] or an Xmon qubit [24–27] with multiple arms capacitively coupled to a coplanar waveguide.

The transmon can be modeled as an anharmonic oscillator [13]. Restricting to the lowest two transmon levels (ground state $|g\rangle$ and excited state $|e\rangle$), the total Hamiltonian for the system is (see Appendix A)

$$H = \hbar\Omega\sigma_+\sigma_- + \int_{-\infty}^{+\infty} dk\, \hbar\omega_k \hat{a}_k^\dagger \hat{a}_k + \sum_{m=1}^{N}\int_{-\infty}^{\infty} g_0(e^{ikx_m}\hat{a}_k\sigma_+ + \text{H.c.})\sqrt{|k|}dk, \quad (1)$$

where Ω is the atomic transition frequency and we have defined the atomic operators $\sigma_+ \equiv |e\rangle\langle g|$ and $\sigma_- \equiv |g\rangle\langle e|$. The parameters k, v, and $\omega_k = |k|v$ are the wave vectors, velocities, and frequencies of the bosonic fields (phonons or photons) in the waveguide. The field operators $\hat{a}_k$ satisfy $[\hat{a}_k, \hat{a}_{k'}^\dagger] = \delta(k - k')$. The rotating-wave approximation (RWA) has been applied in the interaction term. The coupling strength g_0 at each coupling point, located at x_m ($m = 1, 2, \ldots, N$), is measured as an energy density over the wave-vector k space (see Appendix A). We also assume the coupling points are equidistant. Thus, the travel time for bosons between two neighboring coupling points is a constant $\tau = (x_{m+1} - x_m)/v$. In this work, we investigate phenomena arising from non-Markovian dynamics due to τ being non-negligible.

III. EQUATIONS OF MOTION AND THEIR SOLUTIONS

We study the process of spontaneous emission from the giant atom into the waveguide. The atom begins in the excited state $|e\rangle$ and the field in the waveguide is in the vacuum state $|\text{vac}\rangle$. Since the total number of atomic and field excitations is conserved in Eq. (1) due to the RWA, we study the single-excitation subspace of the full system. The total system state can thus be described by

$$|\Psi(t)\rangle = \beta(t)|e, \text{vac}\rangle + \int dk\, \alpha_k(t) a_k^\dagger |g, \text{vac}\rangle, \quad (2)$$

where the integral describes the state of a single boson propagating in the waveguide. From the Schrödinger equation $i\hbar\partial/\partial t|\Psi(t)\rangle = H|\Psi(t)\rangle$, we derive the equation of motion (EOM) for the probability amplitude of the giant atom being excited (see Appendix B):

$$\frac{d}{dt}\beta(t) = -i\Omega\beta(t) - \frac{1}{2}N\gamma\beta(t) - \gamma\sum_{l=1}^{N-1}(N-l)\beta(t-l\tau)\Theta(t-l\tau). \quad (3)$$

Here, the relaxation rate at single coupling point $\gamma \equiv \frac{4\pi g_0^2\Omega}{\hbar^2 v^2}$ can be approximated as a constant over the relevant frequency range in the spirit of Weisskopf-Wigner theory. Note that the EOM (3) also describes the linear (classical) problem where a single harmonic mode, not an atom, interacts with the continuum of modes in an open waveguide. In the harmonic limit of the transmon Hamiltonian, the dynamics of a coherent state (classical motion) exactly follows the EOM (3) for $\beta(t)$ (see Appendix C).

The time evolution of the bosonic field function $\varphi(x,t) \equiv \frac{1}{\sqrt{2\pi}}\int_{-\infty}^{\infty} dk\, e^{ikx}\alpha_k(t)$ in the waveguide is given by (see Appendix B)

$$\varphi(x,t) = -i\sqrt{\frac{\gamma}{2v}}\sum_{m=1}^{N}\beta\left(t - \frac{|x-x_m|}{v}\right)\Theta\left(t - \frac{|x-x_m|}{v}\right). \quad (4)$$

Here, $\Theta(\bullet)$ is the Heaviside step function, which describes time-delayed feedback among the coupling points. The field intensity function $p(x,t) \equiv |\varphi(x,t)|^2$ describes the probability density at position x and time t to find a single phonon or photon for all possible wave vectors k.

The first term on the right-hand side of Eq. (3) describes the coherent dynamics of the atom. The second and third terms describe the relaxation processes due to Markovian and non-Markovian dynamics, respectively. The solution of $\beta(t)$ can be obtained by a Laplace transformation:

$$\beta(t) = \sum_n \frac{e^{s_n t}}{1 - \gamma\tau\sum_{l=1}^{N-1}(N-l)l e^{-s_n l\tau}}, \quad (5)$$

where the complex frequency parameters s_n are given by the solutions to the equation

$$s_n + i\Omega + \frac{1}{2}N\gamma + \gamma\sum_{l=1}^{N-1}(N-l)e^{-s_n l\tau} = 0. \quad (6)$$

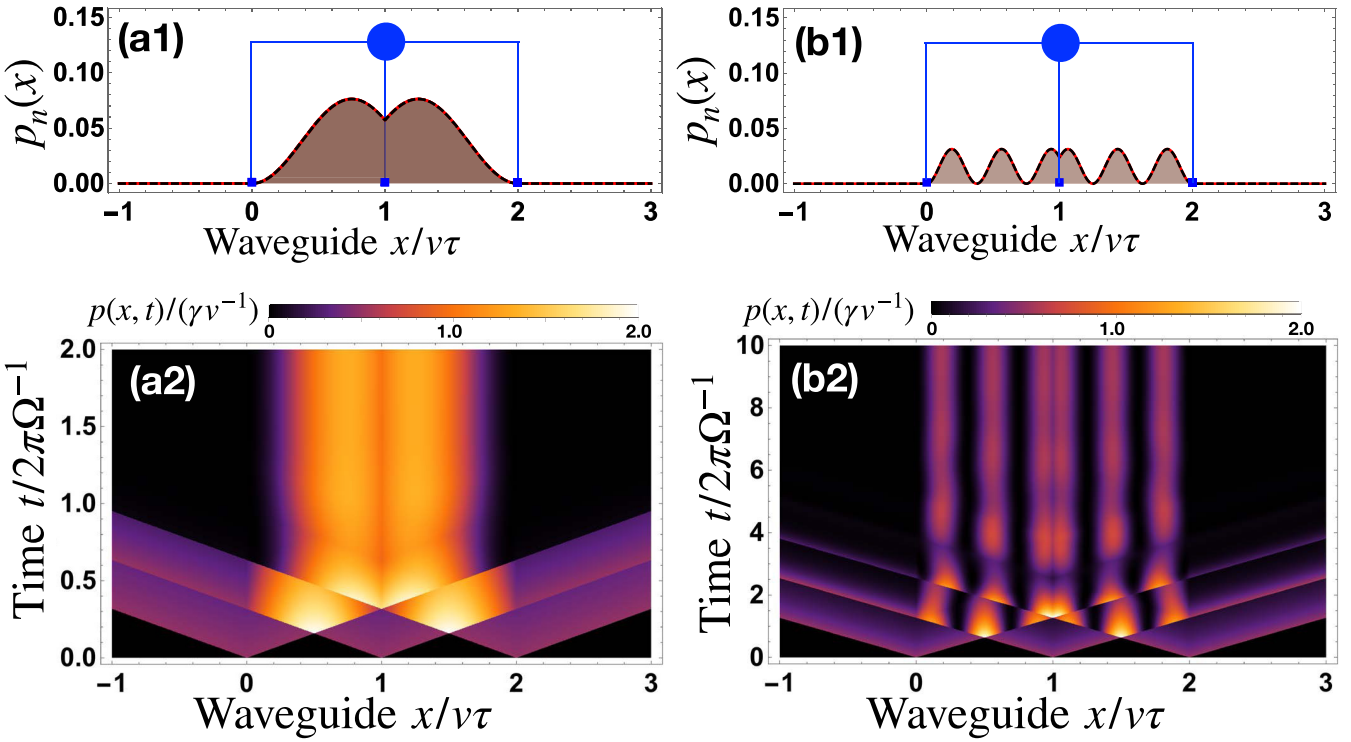

FIG. 2. Bound states in the waveguide for a giant atom with $N = 3$. (a1) Field intensity at $t \to +\infty$ and (a2) field intensity time evolution, for the dark state $s_{n=1}$ with $\gamma\tau/2\pi = 0.018$ and $\Omega\tau/2\pi = 0.317$. In (a1), the red filled curve is the numerical simulation and the black dashed line is the analytical prediction from Eq. (10). (b1), (b2) Same, but for the dark state $s_{n=4}$ with $\gamma\tau/2\pi = 0.073$ and $\Omega\tau/2\pi = 1.27$.

For finite time delay $\tau > 0$, the nonlinear Eq. (6) has multiple solutions. In general, there is no simple closed form for these solutions.

IV. DARK-STATE CONDITION

Usually, the complex frequency s_n has a negative real part, which represents the relaxation rate. In some particular situations, s_n can be purely imaginary. In that case, the corresponding mode is a *dark state*, which does not decay despite the dissipative environment. We seek the purely imaginary solution $s_n \equiv -i\Omega_n$ with (see Appendix D)

$$\Omega_n = \frac{2n\pi}{N\tau}, \quad n \in \mathbb{Z}. \tag{7}$$

Plugging this into Eq. (6), we obtain the following condition for the dark states:

$$\Omega\tau = \frac{2n\pi}{N} - \frac{1}{2}N\gamma\tau \cot\left(\frac{n\pi}{N}\right), \quad n \in \mathbb{Z}. \tag{8}$$

Note that for the RWA to hold, we require $|\Omega_n - \Omega|/\Omega \ll 1$ or, equivalently, $|\frac{N\gamma}{2\Omega}\cot(\frac{n\pi}{N})| \ll 1$ and $n \in \mathbb{Z}^+$ according to Eq. (8). In the Markov limit $\gamma\tau \to 0$, the dark-state condition (8) is simplified into $\Omega\tau = 2n\pi/N$ and the dark frequency is $\Omega_n = \Omega + \frac{1}{2}N\gamma\cot(\frac{n\pi}{N})$ [25]. In the non-Markovian regime of sufficiently large $\gamma\tau$, the additional nonlinear cotangent term in Eq. (8) cannot be neglected. Due to this term, there is an associated bound field state in the waveguide for a given dark state of the atom.

V. STATIC BOUND STATES

Inserting the dark-state solution $s_n = -i\frac{2n\pi}{N\tau}$ into Eq. (5), we obtain the long-time dynamics of the atomic excitation probability amplitude

$$\beta(t) \to A(n)e^{-i\frac{2n\pi}{N\tau}t} \text{ with } A(n) = \frac{2\sin^2(n\pi/N)}{2\sin^2(n\pi/N) + N\gamma\tau}. \tag{9}$$

From Eqs. (4) and (9), we calculate (see Appendix E) the explicit expression for the field density in the long-time limit, $p_n(x) \equiv p(x, t \to \infty)$, for a given dark state s_n:

$$p_n(x) = \frac{8\gamma}{v}\frac{\sin^2\frac{n\pi}{N}\sin^2\left(\frac{n\pi}{N}m'\right)}{\left(2\sin^2\frac{n\pi}{N} + N\gamma\tau\right)^2}\sin^2\left[\frac{n\pi}{N}(m' + 2\lambda - 1)\right]. \tag{10}$$

Here, we have relabeled the position coordinate by $x = (m' - 1 + \lambda)v\tau$ with $m' = 1, 2, \ldots, N$ and $\lambda \in [0, 1)$. Equation (10) is only valid for the position between the two outermost coupling points, i.e., $x \in [x_1, x_N]$ with $x_1 = 0$ and $x_N = (N - 1)v\tau$. Outside the giant atom, i.e., for $x \notin [x_1, x_N]$, the field intensity $p_n(x)$ is zero.

We calculate [65] the total field intensity $I(n)$ of the bound field state for a given dark state:

$$I(n) \equiv \int p_n(x)dx = \frac{2N\gamma\tau\sin^2\frac{n\pi}{N}}{\left(2\sin^2\frac{n\pi}{N} + N\gamma\tau\right)^2} \times \left(1 + \frac{N}{4n\pi}\sin\frac{2n\pi}{N}\right). \tag{11}$$

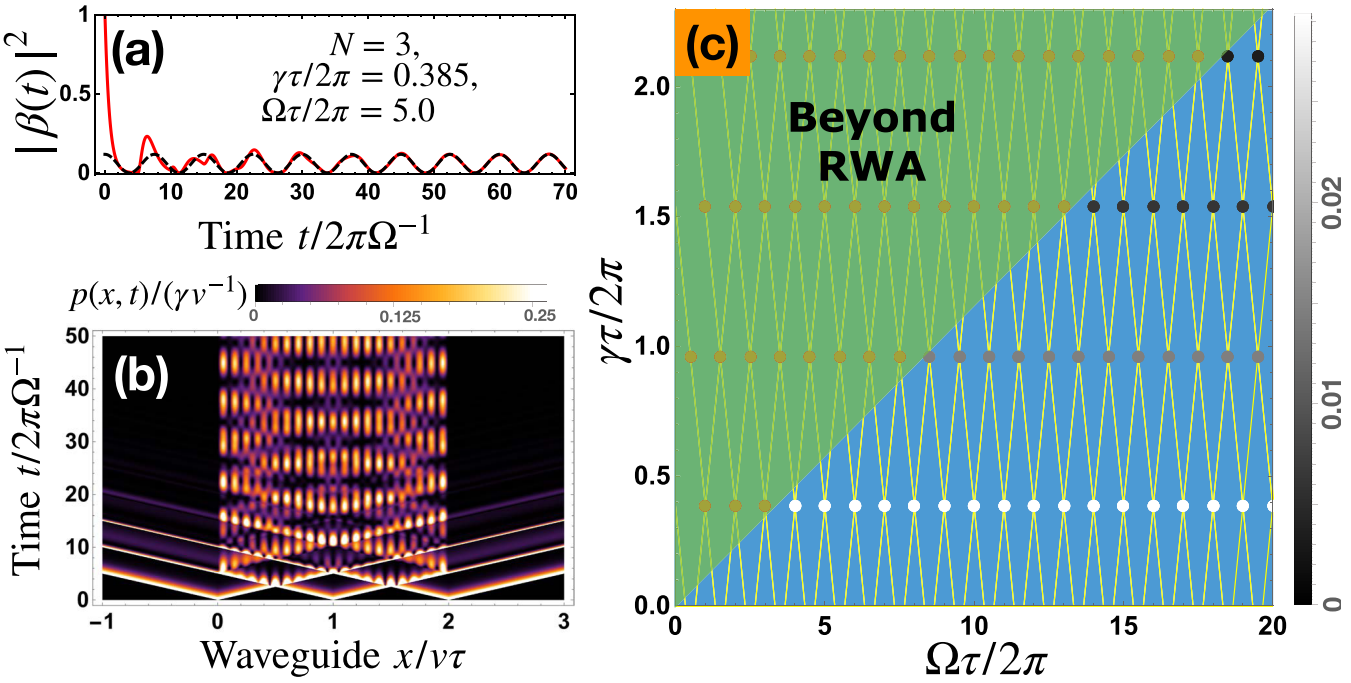

FIG. 3. Oscillating bound states for a giant atom with $N = 3$. (a) Time evolution of the atomic excitation probability $|\beta(t)|^2$ with two coexisting dark states $s_{n=14}$ and $s_{n=16}$, from the numerical simulation (red solid line) and the analytical result (black dashed line) of Eq. (14). (b) Time evolution of the field intensity $p(x,t)$ in the waveguide with the same parameters as in (a). (c) Conditions for oscillating bound states (solid dots) in the $\Omega\tau$-$\gamma\tau$ parameter plane. The gray color level of the dots in the RWA region indicates the oscillating amplitude of $A(n_1)A(n_2)$. The yellow lines show the conditions for nonoscillating bound states (as in Fig. 2) from Eq. (8) with fixed integers $n \in \mathbb{Z}^+$.

We see that, in the Markovian limit $\gamma\tau \to 0$, the total field strength $I(n) \to 0$. Thus, the bound state only exists in the non-Markovian regime, where $\gamma\tau$ is sufficiently large. In the special case of $N = 2$, the dark-state condition (8) can only be fulfilled for odd integers n, and the residual field strength is $I(n) = \gamma\tau/(1+\gamma\tau)^2 \leqslant 1/4$. In Fig. 2, we show how the bound state is formed. We plot the long-time field intensity distribution $p_n(x)$ [Figs. 2(a1) and 2(b1)] and the time evolution of the field intensity function $p(x,t)$ [Figs. 2(a2) and 2(b2)] for two different dark states ($n = 1$ and 4) of a giant atom with $N = 3$ coupling points.

VI. OSCILLATING BOUND STATES

The dark-state condition (8) is a nonlinear equation for integer n and $\gamma\tau > 0$. It is possible to find two integers n_1 and n_2 satisfying Eq. (8) simultaneously. This means that, in the long-time limit after all the dissipative modes die out, the dynamics of the atomic excitation probability amplitude $\beta(t)$ is a superposition of two dark states with different frequencies Ω_{n_1} and Ω_{n_2}. As a result, the atomic excitation probability $|\beta(t)|^2$ oscillates persistently with frequency $\Omega_{n_1} - \Omega_{n_2}$ despite the dissipative environment. In Fig. 3(a), we show the population dynamics for a three-leg giant atom ($N = 3$) with two coexisting dark states: $s_{n=14}$ and $s_{n=16}$. The undamped oscillation of $|\beta(t)|^2$ indicates that the atom exchanges energy with the bosonic bath persistently. In Fig. 3(b), we plot the corresponding time evolution of the field intensity in the waveguide, showing an oscillating bound state in the long-time limit [65].

If n_1 and n_2 are the two simultaneous solutions of Eq. (8), the parameters $\Omega\tau$ and $\gamma\tau$ have to be

$$\Omega\tau = \frac{2n_1\pi}{N} - \frac{2(n_1-n_2)\pi}{N}\frac{\cot\left(\frac{n_1\pi}{N}\right)}{\cot\left(\frac{n_1\pi}{N}\right) - \cot\left(\frac{n_2\pi}{N}\right)} > 0,$$
$$\gamma\tau = \frac{4(n_1-n_2)\pi}{N^2}\frac{1}{\cot\left(\frac{n_1\pi}{N}\right) - \cot\left(\frac{n_2\pi}{N}\right)} > 0. \tag{12}$$

Here, the physical conditions of $\Omega\tau > 0$ and $\gamma\tau > 0$ need to be satisfied, together with the RWA condition that $|\frac{N\gamma}{2\Omega}\cot(\frac{n_{1(2)}\pi}{N})| \ll 1$ and $n_{1(2)} \in \mathbb{Z}^+$. The long-time dynamics of the giant atom is

$$\beta(t) \to A(n_1)e^{-i\Omega_{n_1}t} + A(n_2)e^{-i\Omega_{n_2}t}, \tag{13}$$

which results in

$$|\beta(t)|^2 = A^2(n_1) + A^2(n_2) + 2A(n_1)A(n_2)\cos[(\Omega_{n_1} - \Omega_{n_2})t]. \tag{14}$$

The amplitude of the persistent oscillations is thus $A(n_1)A(n_2)$.

The total field intensity left in the waveguide for two coexisting dark states is $I(n_1,n_2) \equiv \int p(x, t\to\infty)dx$, which can be calculated from Eqs. (4) and (5) (see Appendix F):

$$I(n_1,n_2) = I(n_1) + I(n_2) - 4A(n_1)A(n_2) \times \frac{\Omega\cos[(\Omega_{n_1} - \Omega_{n_2})t]}{\Omega_{n_1} + \Omega_{n_2}}. \tag{15}$$

According to Eq. (2), the quantity $|\beta(t)|^2 + I(n_1,n_2)$ is the total excitation probability of the atom and the field, which is

conserved, since the oscillating bound state does not decay. This gives an additional condition for the coexisting dark states, i.e.,

$$\frac{\Omega_{n_1} + \Omega_{n_2}}{2} = \Omega. \tag{16}$$

Combining this with Eq. (8), we find that the solutions are of the form $n_1 = pN + n$ and $n_2 = qN - n$ with $p, q \in \mathbb{Z}^+$ and $1 \leqslant n < N$. The conditions in Eq. (12) then become $\Omega\tau/2\pi = (p+q)/2$ and $\gamma\tau/2\pi = [(p-q)/N + 2n/N^2]\tan(\frac{n\pi}{N})$. By setting $p \geqslant q$ and $1 \leqslant n < N/2$, Eq. (12) can be satisfied and we obtain the frequencies of the two dark modes: $\Omega \pm \frac{1}{2}N\gamma\cot(\frac{n\pi}{N})$.

In Fig. 3(c), we show the existence of oscillating bound states (solid dots) in the $\Omega\tau$-$\gamma\tau$ parameter space for a giant atom with $N = 3$. The condition in Eq. (12) implies that, if n_1 and n_2 are solutions yielding coexisting dark states, the integers $n_1 + N$ and $n_2 + N$ are also solutions of coexisting dark states with $\gamma\tau$ unchanged but $\Omega\tau$ increased by 2π. This results in the 2π periodicity along the horizontal direction in Fig. 3(c). The dots in the green region are beyond RWA, where the dark-mode frequency $|\Omega_{n_{1(2)}} - \Omega|/\Omega > 0.1$.

If the giant atom only has two coupling points ($N = 2$), the nonlinear cotangent term in condition (8) is either zero or infinity. Therefore, *the oscillating bound states only exist for more than two coupling points ($N \geqslant 3$).*

VII. CONTINUUM LIMIT

We now discuss the limit of infinitely many coupling points ($N \to \infty$). In this case, the time it takes for the field to pass all coupling points is $N\tau \to T$. For capacitive coupling between the atom and the waveguide, the interaction strength g at a single point is proportional to the local capacitance c, i.e., $g \propto c$ [13,16] and the relaxation rate is $\gamma \propto g^2 \propto c^2$ [25,63]. As a result, the parameter $N^2\gamma \propto (Nc)^2$, where Nc is the total capacitance, is a converged quantity $N^2\gamma \to \Gamma$ describing the total relaxation rate of the atom into the waveguide. In this continuum limit, the dark-state condition (8) becomes

$$\Omega T = 2n\pi - \frac{\Gamma T}{2n\pi}, \quad n \in \mathbb{Z}. \tag{17}$$

The solution is $n = (4\pi)^{-1}[\Omega T \pm \sqrt{(\Omega T)^2 + 4\Gamma T}] \in \mathbb{Z}$, and the corresponding dark-mode frequency is $\Omega_n = \Omega + \frac{\Gamma}{2n\pi}$. The field intensity $p_n(x)$ of the bound state can be calculated from Eq. (10), yielding

$$p_n(x) = \frac{2n^2\pi^2/\Gamma T}{(2n^2\pi^2/\Gamma T + 1)^2}\frac{4}{L}\sin^4\left(\frac{n\pi}{L}x\right), \tag{18}$$

where $L = x_N - x_1$. The total field intensity is

$$I(n) = (3n^2\pi^2/\Gamma T)(2n^2\pi^2/\Gamma T + 1)^{-2} \leqslant 3/8.$$

However, since the RWA condition requires $n > 0$, and we only have one solution fulfilling that condition, it is not expected that an oscillating bound state can be created in this case.

As discussed below EOM (3), our predictions also apply to the linear (classical) system of a single harmonic oscillator coupled to an open waveguide. In Fig. 4(a), we show a continuum metal contacting capacitively with an infinite

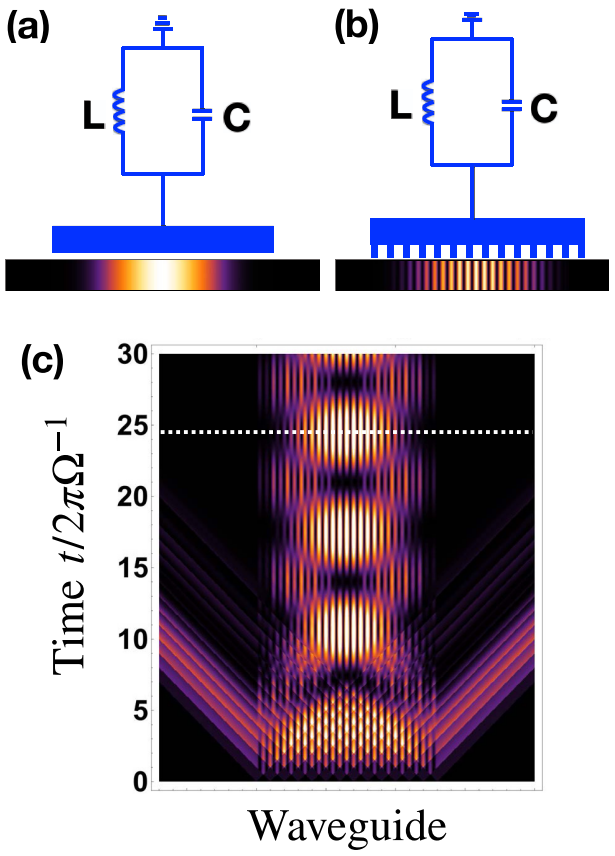

FIG. 4. Sketch for generating (a) a static bound state with a continuum metal and (b) an oscillating bound state with a comblike metal. The colors in the waveguides show the field intensity of the bound states. In (b), the field intensity is taken at the fixed moment indicated by the white dashed line on the plot of $p(x,t)$ in (c). LC circuits are used to tune the plasmon frequency Ω in the metal. Parameters: (a) $n = 1$; (b) and (c) $\Omega\tau = 2\pi$, $\Gamma T \to 4\pi^2$ (i.e., $n = 1$).

SAW waveguide made of piezoelectric material. The metal is attached to an LC circuit to tune the plasmon frequency in the metal. If the dark-state condition (17) is satisfied, we expect to observe a bound state in the waveguide. To generate an oscillating bound state, we can design the contact part of the metal as a comblike structure as shown in Fig. 4(b). Note that the two integers $n_1 = N + n$ and $n_2 = N - n$ with $1 \leqslant n < N/2$ always satisfy the dark-state condition (12). In the limit of infinitely many coupling points $N \gg n$, i.e., for a very extended comb, we have $\Omega\tau = 2\pi$ and $\Gamma T \to (2n\pi)^2$. In this parameter setting, we can create two coexisting dark modes with frequencies $\Omega_\pm \to \Omega \pm \frac{\Gamma}{2\pi n}$. We show the field intensity of bound states in the 1D waveguide for the dark state $n = 1$ in Figs. 4(b) and 4(c).

VIII. DISCUSSION AND CONCLUSION

We have shown that a giant atom with $N \geqslant 3$ coupling points to an open waveguide can harbor *oscillating bound states*. To observe these states in experiment, the coherence time of the (artificial) atom must exceed the oscillation period. For a transmon or Xmon qubit, the coherence time can be on the order of hundreds of microseconds [7,24,66–68], which

is much longer than the oscillation period shown in Fig. 3(a) since, typically, $\Omega/2\pi$ is several gigahertz.

In contrast to bound states arising from an impurity protected by an energy gap [51–58], the bound states we find here appear inside the continuous energy spectrum. Therefore, it is possible to manipulate (catch or release) propagating photons/phonons in the waveguide by tuning the dark-mode condition [Eq. (8)] [69]. Furthermore, since the oscillating bound states are a result of coexisting bound modes, their Hilbert space is larger than those of previously known bound states, which should enable storage and manipulation of more complex quantum states. Note that the total amount of excitation stored in the (oscillating) bound state given by Eqs. (11) and (15) depends on the integer n, which can be changed by detuning the atomic transition frequency Ω. Finally, the oscillating bound state, i.e., the dynamical exchange of excitations between the atom and the bosonic field, essentially demonstrates the Rabi-oscillation phenomenon of cavity QED (undamped, unlike in Ref. [64]). Typically, cavity QED requires two mirrors (which could be atoms [70]) or a segmented waveguide serving as a cavity, but this shows that a single giant atom with three coupling points in the open waveguide is a minimalistic implementation of cavity QED.

ACKNOWLEDGMENTS

A.F.K. acknowledges support from the Swedish Research Council (Grant No. 2019-03696). A.F.K. and G.J. acknowledge support from the Knut and Alice Wallenberg Foundation through the Wallenberg Centre for Quantum Technology (WACQT).

APPENDIX A: HAMILTONIAN

The transmon is coupled capacitively to the waveguide. The total Hamiltonian of the transmon coupled to a waveguide is given by [13]

$$\begin{aligned} H_{\rm tr} &= \frac{(2e)^2}{2C_\Sigma}(\hat{n}-\hat{n}_s)^2 - E_J\cos\hat{\varphi} \\ &\equiv 4E_C\hat{n}^2 - E_J\cos\hat{\varphi} - 8E_C\hat{n}\hat{n}_s + 4E_C\hat{n}_s^2, \end{aligned} \tag{A1}$$

where $\hat{n}_s$ is the offset charge of the transmon measured in units of the Cooper pair charge $2e$, E_J is the Josephson energy, and $E_C = e^2/2C_\Sigma$ is the charging energy with C_Σ the total capacitance of the transmon. By defining the operators $\hat{b}$, $\hat{b}^\dagger$ via $\hat{\varphi} = \sqrt{\frac{\eta}{2}}(\hat{b}+\hat{b}^\dagger)$, $\hat{n} = -i\sqrt{\frac{1}{2\eta}}(\hat{b}-\hat{b}^\dagger)$ with $\eta \equiv \sqrt{8E_C/E_J}$, the free transmon Hamiltonian is

$$H_{\rm tr,free} = 4E_C\hat{n}^2 - E_J\cos\hat{\varphi} \approx \hbar\omega_0\left(\hat{b}^\dagger\hat{b}+\tfrac{1}{2}\right) - \chi(\hat{b}+\hat{b}^\dagger)^4, \tag{A2}$$

where $\omega_0 = \sqrt{8E_CE_J}/\hbar$ is known as the Josephson plasma frequency and $\chi = E_C/12$ is the nonlinearity.

The electric potential field $\phi(x,t)$ in the waveguide can be described by [71]

$$\hat{\phi}(x,t) = -i\sqrt{\frac{\hbar Z_0 v}{4\pi}}\int_{-\infty}^{\infty} dk\sqrt{\omega_k}(\hat{a}_k e^{-i(\omega_k t-kx)} - \text{H.c.}). \tag{A3}$$

Here, $\hat{a}_k$ is the annihilation operator of the waveguide mode with wave vector k, satisfying the commutation relations $[\hat{a}_k, \hat{a}_{k'}^\dagger] = \delta(k-k')$, Z_0 is the characteristic impedance of the waveguide, and v is the velocity of SAWs or the speed of light (microwaves) with the dispersion relation $\omega_k = |k|v$.

The coupling between the transmon and the waveguide is described by the term $H_{\rm int} = -8E_C\hat{n}\hat{n}_s$ in Eq. (A1) with the offset charge $\hat{n}_s = (2e)^{-1}\sum_{m=1}^N C_g\hat{\phi}(x_m,t)$, where C_g and x_m are the effective capacitance and the position of each coupling point, respectively. Therefore, the interaction Hamiltonian is

$$\begin{aligned} H_{\rm int} &= -8E_C\hat{n}\hat{n}_s \\ &= -i8E_C\sqrt{\frac{1}{2\eta}}(\hat{b}-\hat{b}^\dagger)\frac{1}{2e}\sum_{m=1}^N C_g\hat{\phi}(x_m,t) \\ &= \frac{4E_C}{e}\sqrt{\frac{1}{2\eta}}\sqrt{\frac{\hbar Z_0 v}{4\pi}} \\ &\times \sum_{m=1}^N C_g\int_{-\infty}^{\infty} dk\sqrt{\omega_k}(\hat{a}_k e^{ikx_m} - \text{H.c.})(\hat{b}^\dagger - \hat{b}) \\ &\approx \frac{4E_C}{e}\sqrt{\frac{1}{2\eta}}\sqrt{\frac{\hbar Z_0 v}{4\pi}}\sum_{m=1}^N C_g \\ &\quad\times \int_{-\infty}^{\infty} dk\sqrt{|k|v}(\hat{b}^\dagger\hat{a}_k e^{ikx_m} + \text{H.c.}) \\ &= \sum_{m=1}^N\int_{-\infty}^{\infty} g_0(\hat{b}^\dagger\hat{a}_k e^{ikx_m} + \text{H.c.})\sqrt{|k|}dk. \end{aligned} \tag{A4}$$

In the fourth line, we used the linear dispersion relation $\omega_k = v|k|$ and adopted the rotating-wave approximation (RWA) by dropping counter-rotating terms like $\hat{a}_k^\dagger\hat{b}^\dagger$ and $\hat{a}_k\hat{b}$. In the fifth line, we defined the coupling strength

$$g_0 \equiv \frac{4E_C}{e}v\sqrt{\frac{1}{2\eta}}\sqrt{\frac{\hbar Z_0}{4\pi}}C_g. \tag{A5}$$

Note that the coupling strength g_0 is measured as an energy density over the wave-vector k space since we are considering continuous modes in the open waveguide.

Thus, the total Hamiltonian including the waveguide is

$$\begin{aligned} H &= \hbar\omega_0\left(\hat{b}^\dagger\hat{b}+\frac{1}{2}\right) - \chi(\hat{b}+\hat{b}^\dagger)^4 + \int_{-\infty}^{+\infty} dk\,\hbar\omega_k\hat{a}_k^\dagger\hat{a}_k \\ &+ \sum_{m=1}^N\int_{-\infty}^{\infty} g_0(\hat{b}^\dagger\hat{a}_k e^{ikx_m} + \text{H.c.})\sqrt{|k|}dk. \end{aligned} \tag{A6}$$

APPENDIX B: SINGLE-EXCITATION LIMIT

For the spontaneous emission process, the RWA guarantees that there is only one excitation either in the atomic state or in the waveguide. In this case, only the lowest two levels of the transmon, i.e., the ground state $|g\rangle$ and the first excited state $|e\rangle$, are involved in the dynamics. By defining the lowering operator $\sigma_- \equiv |g\rangle\langle e|$ and raising operator $\sigma_+ \equiv |e\rangle\langle g|$, we can

write the Hamiltonian in the single-excitation subspace

$$H = \hbar\Omega\sigma_+\sigma_- + \int_{-\infty}^{+\infty} dk\, \hbar\omega_k \hat{a}_k^\dagger \hat{a}_k + \sum_{m=1}^{N}\int_{-\infty}^{\infty} g_0(e^{ikx_m}\hat{a}_k\sigma_+ + \text{H.c.})\sqrt{|k|}dk. \quad \text{(B1)}$$

Here, the atomic transition frequency $\Omega = \omega_0 - 12\chi = \sqrt{8E_C E_J}/\hbar - E_C/\hbar$ is the level spacing of the two lowest levels. The total system state can thus be described by

$$|\Psi(t)\rangle = \beta(t)|e, \text{vac}\rangle + \int dk\, \alpha_k(t)\hat{a}_k^\dagger|g, \text{vac}\rangle, \quad \text{(B2)}$$

where the integral describes the state of a single boson propagating in the waveguide. From the Schrödinger equation $i\hbar\partial/\partial t|\Psi(t)\rangle = H|\Psi(t)\rangle$, we have

$$\begin{aligned} &H|\Psi(t)\rangle \\ &= \hbar\Omega\beta(t)|e, \text{vac}\rangle + \hbar\int dk\, \omega_k\alpha_k(t)\hat{a}_k^\dagger|g, \text{vac}\rangle \\ &\quad + \beta(t)\sum_{m=1}^{N}\int_{-\infty}^{\infty} g_0\sqrt{|k|}e^{-ikx_m}\hat{a}_k^\dagger|g, \text{vac}\rangle dk \\ &\quad + \sum_{m=1}^{N}\int_{-\infty}^{\infty} g_0\sqrt{|k|}e^{ikx_m}\alpha_k(t)|e, \text{vac}\rangle dk \\ &= i\hbar\frac{d}{dt}\beta(t)|e, \text{vac}\rangle + i\hbar\int dk\frac{d}{dt}\alpha_k(t)\hat{a}_k^\dagger|g, \text{vac}\rangle. \end{aligned} \quad \text{(B3)}$$

Therefore, the dynamics for the giant atom is

$$\frac{d}{dt}\beta(t) = -i\Omega\beta(t) - i\frac{g_0}{\hbar}\sum_{m=1}^{N}\int_{-\infty}^{\infty}\sqrt{|k|}e^{ikx_m}\alpha_k(t)dk \quad \text{(B4)}$$

and for the propagating modes in the waveguide

$$\frac{d}{dt}\alpha_k(t) = -i\omega_k\alpha_k(t) - i\frac{g_0}{\hbar}\beta(t)\sqrt{|k|}\sum_{m=1}^{N}e^{-ikx_m}. \quad \text{(B5)}$$

Integrating Eq. (B5), we have the formal solution

$$\alpha_k(t) = e^{-i\omega_k t}\left\{\alpha_k(0) - i\frac{g_0}{\hbar}\sqrt{|k|}\sum_{m=1}^{N}e^{-ikx_m}\int_0^t\beta(t')e^{i\omega_k t'}dt'\right\}. \quad \text{(B6)}$$

Inserting Eq. (B6) into Eq. (B4), we obtain

$$\begin{aligned} \frac{d}{dt}\beta(t) &= -i\Omega\beta(t) - \left(\frac{g_0}{\hbar}\right)^2\sum_{m,m'=1}^{N}\int_0^t\beta(t')dt'\int_{-\infty}^{\infty}|k|e^{ik(x_m-x_{m'})+i\omega_k(t'-t)}dk - i\frac{g_0}{\hbar}\sum_{m=1}^{N}\int_{-\infty}^{\infty}\sqrt{|k|}e^{i(kx_m-\omega_k t)}\alpha_k(0)dk \\ &= -i\Omega\beta(t) - \left(\frac{g_0}{\hbar v}\right)^2\sum_{m,m'=1}^{N}\int_0^t\beta(t')dt'\int_0^{\infty}\omega_k\left[e^{i\omega_k(x_m-x_{m'})/v+i\omega_k(t'-t)} + e^{i\omega_k(x_{m'}-x_m)/v+i\omega_k(t'-t)}\right]d\omega_k \\ &\quad -i\frac{g_0}{\hbar v}\sum_{m=1}^{N}\int_{-\infty}^{\infty}\sqrt{\omega_k}e^{i(kx_m-\omega_k t)}\alpha_k(0)dk. \end{aligned} \quad \text{(B7)}$$

In order to simplify Eq. (B7), we adopt the well-known Weisskopf-Wigner approximation [72]. In the emission spectrum, the intensity of the emitted radiation is concentrated in the range around the atomic transition frequency Ω. Therefore, the quantity ω_k varies little in this frequency range, and we define the relaxation rate at single coupling point by

$$\gamma \equiv \frac{4\pi g_0^2\Omega}{\hbar^2 v^2} \approx \text{constant}. \quad \text{(B8)}$$

We can replace the lower limit in the ω_k integration by $-\infty$ in Eq. (B7). The integral $\int_{-\infty}^{+\infty}d\omega_k e^{i\omega_k t} = 2\pi\delta(t)$ yields

$$\begin{aligned} \frac{d}{dt}\beta(t) &\approx -i\Omega\beta(t) - \frac{\gamma}{2}\sum_{m,m'=1}^{N}\int_0^t\beta(t')dt'[\delta(t'-t+\tau_{mm'}) + \delta(t'-t-\tau_{mm'})] - i\sqrt{\frac{\gamma v}{4\pi}}\sum_{m=1}^{N}\int_{-\infty}^{\infty}e^{i(kx_m-\omega_k t)}\alpha_k(0)dk \\ &= -i\Omega\beta(t) - \frac{\gamma}{2}\sum_{m,m'=1}^{N}\beta(t-|\tau_{mm'}|)\Theta(t-|\tau_{mm'}|) - i\sqrt{\frac{\gamma v}{4\pi}}\sum_{m=1}^{N}\int_{-\infty}^{\infty}e^{i(kx_m-\omega_k t)}\alpha_k(0)dk, \end{aligned} \quad \text{(B9)}$$

where we have defined the delay time $\tau_{mm'} \equiv (x_m - x_{m'})/v$ between two coupling points and $\Theta(x)$ is the Heaviside step function [$\Theta(x) = 0$ for $x < 0$ and $\Theta(x) = 1$ for $x > 0$]. We make the Markovian approximation at each single coupling point but retain the time delay (non-Markovian dynamics) between different coupling points.

Since each $\alpha_k(t)$ represents the time-dependent probability amplitude of a plane wave e^{ikx}, the total time-dependent field function in the waveguide is given by

$$\varphi(x,t) \equiv \frac{1}{\sqrt{2\pi}} \int_{-\infty}^{\infty} dk\, e^{ikx} \alpha_k(t). \tag{B10}$$

From Eq. (B6), we have

$$\begin{aligned}\varphi(x,t) &= \frac{1}{\sqrt{2\pi}} \int_{-\infty}^{\infty} dk\, e^{i(kx-\omega_k t)} \alpha_k(0) - i\frac{1}{\sqrt{2\pi}} \sqrt{\frac{\gamma v}{4\pi}} \sum_{m=1}^{N} \int_0^t \beta(t')dt' \int_{-\infty}^{\infty} dk\, e^{ik(x-x_m)+i\omega_k(t'-t)} \\ &\approx \frac{1}{\sqrt{2\pi}} \int_{-\infty}^{\infty} dk\, e^{i(kx-\omega_k t)} \alpha_k(0) - i\sqrt{\frac{\gamma}{2v}} \sum_{m=1}^{N} \beta\left(t - \frac{|x-x_m|}{v}\right) \Theta\left(t - \frac{|x-x_m|}{v}\right).\end{aligned} \tag{B11}$$

In the last step, we used the Weisskopf-Wigner approximation again like we did in Eq. (B9).

In order to solve Eq. (B9), we use Laplace transformation $E_\beta(s) \equiv \int_0^\infty dt\, \beta(t) e^{-st}$ and obtain

$$sE_\beta(s) - \beta(0) = -i\Omega E_\beta(s) - \frac{\gamma}{2} \sum_{m,m'=1}^{N} e^{-|\tau_{mm'}|s} E_\beta(s) - i\sqrt{\frac{\gamma v}{4\pi}} \sum_{m=1}^{N} \int_{-\infty}^{\infty} \frac{e^{ikx_m} \alpha_k(0)}{s + i\omega_k} dk. \tag{B12}$$

Therefore, we have

$$E_\beta(s) = \frac{\beta(0)}{s + i\Omega + \frac{\gamma}{2}\sum_{m,m'=1}^{N} e^{-|\tau_{mm'}|s}} - i\sqrt{\frac{\gamma v}{4\pi}} \sum_{m=1}^{N} \int_{-\infty}^{\infty} \frac{e^{ikx_m} \alpha_k(0)}{(s + i\Omega + \frac{\gamma}{2}\sum_{m,m'=1}^{N} e^{-|\tau_{mm'}|s})(s + i\omega_k)} dk. \tag{B13}$$

The time evolution of $\beta(t)$ can be obtained by the inverse Laplace transformation

$$\beta(t) = \sum e^{s_{\text{pole}} t} \text{Res}(E_\beta(s), s_{\text{pole}}) = \sum e^{s_{\text{pole}} t} \lim_{s \to s_{\text{pole}}} E_\beta(s)(s - s_{\text{pole}}) = \sum e^{s_{\text{pole}} t} \lim_{\epsilon \to 0} E_\beta(s_{\text{pole}} + \epsilon)\epsilon, \tag{B14}$$

where $\text{Res}(E_\beta(s), s_{\text{pole}})$ is the residue of $E_\beta(s)$ at the pole s_{pole}. The poles of $E_\beta(s)$ are $s_{\text{pole}} = -i\omega_k$ and also given by the roots of the following equation:

$$s_n + i\Omega + \frac{\gamma}{2} \sum_{m,m'=1}^{N} e^{-|\tau_{mm'}|s_n} = 0. \tag{B15}$$

The explicit form of $\beta(t)$ is thus

$$\begin{aligned}\beta(t) = &\sum_n \frac{\beta(0) e^{s_n t}}{1 - \frac{\gamma}{2}\sum_{m,m'=1}^{N} |\tau_{mm'}| e^{-|\tau_{mm'}|s_n}} - i\sqrt{\frac{\gamma v}{4\pi}} \sum_{m=1}^{N} \int_{-\infty}^{\infty} \frac{\alpha_k(0) e^{ikx_m - i\omega_k t}}{i(\Omega - \omega_k) + \frac{\gamma}{2}\sum_{m,m'=1}^{N} e^{i\omega_k|\tau_{mm'}|}} dk \\ &- i\sqrt{\frac{\gamma v}{4\pi}} \sum_n \sum_{m=1}^{N} \int_{-\infty}^{\infty} \frac{\alpha_k(0) e^{ikx_m + s_n t}}{(1 - \frac{\gamma}{2}\sum_{m,m'=1}^{N} |\tau_{mm'}| e^{-|\tau_{mm'}|s_n})(s_n + i\omega_k)} dk.\end{aligned} \tag{B16}$$

If the pole from Eq. (B15) is a purely imaginary number, i.e., $s_n = -i\omega_k$, the k-component contribution in the integration of Eq. (B16) is zero.

In our experimental scheme proposed in the main text, the coupling points are equidistant with time delay τ between neighboring points. Therefore, all the possible time delays can be written on the form $|\tau_{mm'}| = l\tau$ with $l = 0, 1, \ldots, N-1$. The combination number of time delays is N for $l = 0$ and $2(N-l)$ for $l \neq 0$. Therefore, the condition (B15) to determine the poles becomes

$$s_n + i\Omega + \frac{1}{2}N\gamma + \gamma \sum_{l=1}^{N-1} (N-l) e^{-s_n l\tau} = 0, \tag{B17}$$

which is Eq. (6) in the main text. In this case, the EOM (B9) for $\beta(t)$ becomes

$$\begin{aligned}\frac{d}{dt}\beta(t) = &-i\Omega\beta(t) - \frac{1}{2}N\gamma\beta(t) - \gamma \sum_{l=1}^{N-1} \beta(t - l\tau)\Theta(t - l\tau) \\ &-i\sqrt{\frac{\gamma v}{4\pi}} \sum_{m=1}^{N} \int_{-\infty}^{\infty} e^{i(kx_m - \omega_k t)} \alpha_k(0) dk,\end{aligned} \tag{B18}$$

which is Eq. (3) in the main text. For the spontaneous emission $\alpha_k(0) = 0$ and $\beta(0) = 1$, the solution (B16) by Laplace transformation is

$$\beta(t) = \sum_n \frac{e^{s_n t}}{1 - \gamma\tau \sum_{l=1}^{N-1} (N-l) e^{-s_n l\tau}}, \tag{B19}$$

which is Eq. (5) in the main text.

APPENDIX C: HARMONIC LIMIT

In the harmonic limit, where the nonlinearity vanishes $\chi \to 0$, the total Hamiltonian (A6) becomes

$$H = \hbar\Omega\hat{b}^\dagger\hat{b} + \int_{-\infty}^{+\infty} dk\, \hbar\omega_k \hat{a}_k^\dagger \hat{a}_k + \sum_{m=1}^{N}\int_{-\infty}^{\infty} g_0(e^{ikx_m}\hat{a}_k\hat{b}^\dagger + \text{H.c.})\sqrt{|k|}dk. \quad \text{(C1)}$$

The Heisenberg EOM for the transmon operator $\hat{b}(t)$ is

$$\frac{d}{dt}\hat{b}(t) = \frac{1}{i\hbar}[\hat{b}(t), H(t)] = -i\Omega\hat{b}(t) - i\frac{g_0}{\hbar}\sum_{m=1}^{N}\int_{-\infty}^{\infty}\sqrt{|k|}e^{ikx_m}\hat{a}_k dk. \quad \text{(C2)}$$

The Heisenberg EOM for the field operator $\hat{a}_k(t)$ is

$$\frac{d}{dt}\hat{a}_k(t) = \frac{1}{i\hbar}[\hat{a}_k(t), H(t)] = -i\omega_k\hat{a}_k(t) - i\frac{g_0}{\hbar}\hat{b}(t)\sqrt{|k|}\sum_m e^{-ikx_m}. \quad \text{(C3)}$$

Equations (C2) and (C3) have the exact same form as Eqs. (B4) and (B5) if we replace $\beta(t)$ and $\alpha_k(t)$ by operators $\hat{b}(t)$ and $\hat{a}_k^\dagger$, respectively. Note that the Hamiltonian (C1) describes the linear problem where a single harmonic mode interacts with the continuum of harmonic modes in an open waveguide. If we prepare all the harmonic modes in coherent states initially, they will stay in coherent states with coherent values $\beta(t) = \langle\hat{b}(t)\rangle$ and $\alpha_k(t) = \langle\hat{a}_k(t)\rangle$ described by Eqs. (B4) and (B5). Therefore, the EOM (B9) for the atomic probability amplitude $\beta(t)$ and the EOM (B11) for the single-excitation probability amplitude density $\varphi(x,t)$ also describe the classical dynamics for the complex amplitude of a harmonic mode and the harmonic field function [i.e., $|\varphi(x,t)|^2$ is the field intensity] in the waveguide.

APPENDIX D: SEARCHING FOR DARK MODES

To obtain the explicit solutions for $\beta(t)$, the central problem is to solve Eq. (B17), i.e., find the roots of the transcendental equation

$$s + i\Omega - \frac{1}{2}N\gamma + \gamma\sum_{l=0}^{N-1}(N-l)e^{-sl\tau} = 0. \quad \text{(D1)}$$

It can be proved that

$$G \equiv \sum_{l=0}^{N-1} e^{-sl\tau} = \frac{1-e^{-Ns\tau}}{1-e^{-s\tau}} \quad \text{(D2)}$$

and

$$\sum_{l=0}^{N-1} n e^{-sl\tau} = -\frac{\partial G}{\tau\partial s} = \frac{e^{-s\tau} - Ne^{-Ns\tau} + (N-1)e^{-(N+1)s\tau}}{(1-e^{-s\tau})^2}. \quad \text{(D3)}$$

Thus, we have

$$\sum_{l=0}^{N-1}(N-n)e^{-sl\tau} = N\frac{1-e^{-Ns\tau}}{1-e^{-s\tau}} - \frac{e^{-s\tau} - Ne^{-Ns\tau} + (N-1)e^{-(N+1)s\tau}}{(1-e^{-s\tau})^2} = \frac{N-(N+1)e^{-s\tau} + e^{-(N+1)s\tau}}{(1-e^{-s\tau})^2}. \quad \text{(D4)}$$

Equation (D1) is simplified into

$$s + i\Omega - \frac{1}{2}N\gamma + \gamma\frac{N-(N+1)e^{-s\tau} + e^{-(N+1)s\tau}}{(1-e^{-s\tau})^2} = 0 \quad \text{(D5)}$$

or, multiplied by $\tau(1-e^{-s\tau})^2$,

$$\left[s\tau + i\Omega\tau - \tfrac{1}{2}N\gamma\tau\right](1-e^{-s\tau})^2 + \gamma\tau[N-(N+1)e^{-s\tau} + e^{-(N+1)s\tau}] = 0. \quad \text{(D6)}$$

The solution is determined by the dimensionless parameters $\Omega\tau$, $\gamma\tau$, and N. Although $e^{-s\tau} = 1$ satisfies Eq. (D6), it is *not* the solution of Eq. (D1) since $e^{-s\tau} = 1$ gives $s\tau = -i2n\pi$ with integers n and Eq. (D1) then becomes $i(\Omega\tau - 2n\pi) + \frac{1}{2}N^2\gamma\tau = 0$, which cannot be satisfied for real Ω and finite $\gamma\tau > 0$.

We are interested in searching for the dark states corresponding to a purely imaginary solution s. First, let us check if $s = -i\Omega$ can be the dark mode. In this case, we have from Eq. (D6)

$$2e^{i\Omega\tau}[(e^{i\Omega\tau})^N - 1] - N[(e^{i\Omega\tau})^2 - 1] = 0. \quad \text{(D7)}$$

For *even* integers N, we have the solution $e^{i\Omega\tau} = -1$, indicating that, for even N and $\Omega\tau = (2n+1)\pi$, $s = -i\Omega$ is indeed a dark mode.

To find more dark states, we assume $s = -i\Omega_n$ with a real Ω_n satisfying Eq. (D6). We then have the equation

$$2e^{i\Omega_n\tau}[(e^{i\Omega_n\tau})^N - 1] - N[(e^{i\Omega_n\tau})^2 - 1] = i\frac{2(\Omega_n\tau - \Omega\tau)}{\gamma\tau}(1-e^{i\Omega_n\tau})^2. \quad \text{(D8)}$$

To simplify Eq. (D8) for finding dark states, we make the ansatz that

$$(e^{i\Omega_n\tau})^N = 1 \quad \Rightarrow \quad \Omega_n = \frac{2n\pi}{N\tau}, \quad n \in \mathbb{Z}. \quad \text{(D9)}$$

Thus, we can cancel the first term on the left-hand side of Eq. (D8) and obtain a simplified equation

$$-N[(e^{i\Omega_n\tau})^2 - 1] = i\frac{2(\Omega_n\tau - \Omega\tau)}{\gamma\tau}(1-e^{i\Omega_n\tau})^2 \Rightarrow \frac{1+e^{i\Omega_n\tau}}{1-e^{i\Omega_n\tau}} = i\frac{2(\Omega_n\tau - \Omega\tau)}{N\gamma\tau}. \quad \text{(D10)}$$

Using the identity $(1+e^{i\Omega_n\tau})/(1-e^{i\Omega_n\tau}) = i\cot(\Omega_n\tau/2)$, we have the resonant condition for dark state from the above equation:

$$\Omega\tau = \Omega_n\tau - \frac{1}{2}N\gamma\tau\cot\left(\frac{\Omega_n\tau}{2}\right) = \frac{2n\pi}{N} - \frac{1}{2}N\gamma\tau\cot\left(\frac{n\pi}{N}\right), \quad n \in \mathbb{Z}. \quad \text{(D11)}$$

We label the dark mode by $s_n = -i\Omega_n$ with $\Omega_n = \frac{2n\pi}{N\tau}$, $n \in \mathbb{Z}$. The above Eq. (D11) is the Eq. (8) in the main text.

APPENDIX E: FIELD INTENSITY DISTRIBUTION FOR A SINGLE BOUND STATE

In this Appendix, we derive Eqs. (10) and (11) in the main text. For a given dark mode $s_n = -i\frac{2n\pi}{N\tau}$, the corresponding field intensity can also be calculated from Eqs. (4) and (9) in the main text. By parametrizing the position coordinate as $x = (m'-1)v\tau + \lambda v\tau$ with $m' = 1, 2, \ldots, N$ and $\lambda \in [0, 1)$, we have $p_n(x) = p(x, t \to +\infty)$ and

$$
\begin{aligned}
p(x, t\to+\infty) &= \frac{\gamma}{2v}\left|\sum_m \beta(t-|x-x_m|/v)\Theta(t-|x-x_m|/v)\right|^2 \\
&= \frac{\gamma}{2v}\left(\frac{1}{1+\frac{1}{2}\frac{N\gamma\tau}{\sin^2(n\pi/N)}}\right)^2\left|\sum_m \exp\left[i\frac{2n\pi}{N\tau}\frac{|x-x_m|}{v}\right]\right|^2 \\
&= \frac{\gamma}{2v}\left(\frac{1}{1+\frac{1}{2}\frac{N\gamma\tau}{\sin^2(n\pi/N)}}\right)^2\frac{1}{4}\left|\frac{4}{1-e^{-i\frac{2n\pi}{N}}}\right|^2\left[1-\cos\left(\frac{2n\pi}{N}m'\right)\right]\left[1-\cos\left\{\frac{2n\pi}{N}\left[m'+2\left(\lambda-\frac{1}{2}\right)\right]\right\}\right] \\
&= \frac{\gamma}{2v\sin^2(n\pi/N)}\left(\frac{1}{1+\frac{1}{2}\frac{N\gamma\tau}{\sin^2(n\pi/N)}}\right)^2\left[1-\cos\left(\frac{2n\pi}{N}m'\right)\right]\left[1-\cos\left\{\frac{2n\pi}{N}\left[m'+2\left(\lambda-\frac{1}{2}\right)\right]\right\}\right] \\
&= \frac{2\gamma}{v}\frac{\sin^2\frac{n\pi}{N}}{\left(2\sin^2\frac{n\pi}{N}+N\gamma\tau\right)^2}\left[1-\cos\left(\frac{2n\pi}{N}m'\right)\right]\left[1-\cos\left(\frac{2k\pi}{N}[m'+2\lambda-1]\right)\right] \\
&= \frac{8\gamma}{v}\frac{\sin^2\frac{n\pi}{N}}{\left(2\sin^2\frac{n\pi}{N}+N\gamma\tau\right)^2}\sin^2\left(\frac{n\pi}{N}m'\right)\sin^2\left[\frac{k\pi}{N}(m'+2\lambda-1)\right].
\end{aligned}
\tag{E1}
$$

This distribution is valid for x between x_1 and x_N in the waveguide. We see that at the two ends of the giant atom, $x_1 = 0$ (i.e., $m' = 1$ and $\lambda = 0$) and $x_N = (N-1)v\tau$ (i.e., $m' = N$ and $\lambda = 0$), the intensity vanishes. When the position x is outside the interval $[x_1, x_m]$, since the sign of $(x - x_m)$ is fixed, the summation in the second line gives zero. This is reasonable since the excitations outside the outermost coupling points will propagate away in the waveguide and never come back. The total field intensity left in the waveguide for the given dark state $s_n = -i\frac{2n\pi}{N\tau}$ can be calculated, in the long-time limit, by plugging $\beta(t)$ into the above equation, yielding

$$
\begin{aligned}
I(n) &= \int_{x_1}^{x_N} p_n(x)\,dx \\
&= \frac{\gamma}{2}\left(\frac{1}{1+\frac{1}{2}\frac{N\gamma\tau}{\sin^2(n\pi/N)}}\right)^2\int_0^{\mathcal{T}}\left|\sum_m \exp\left(i\frac{2n\pi}{N\tau}|t'-\tau_m|\right)\right|^2 dt'.
\end{aligned}
\tag{E2}
$$

Here, we have expressed the coordinates in terms of times, i.e., $t' \equiv x/v$ and $\tau_m = (m-1)\tau$ with $m = 1, 2, \ldots, N$. The parameter $\mathcal{T} \equiv (N-1)\tau$ is the total traveling time from x_1 to x_N. By parametrizing $t' = (m'-1)\tau + a\tau$ with $a \in [0, 1)$, we have

$$
\begin{aligned}
\int_0^{\mathcal{T}}\left|\sum_m e^{i\frac{2n\pi}{N\tau}|t'-\tau_m|}\right|^2 dt' &= \tau\sum_{m'=1}^{N}\int_0^1\left|\sum_{m=1}^{m'} e^{i\frac{2n\pi}{N\tau}[(m'-m)\tau+a\tau]} + \sum_{m=m'+1}^{N} e^{i\frac{2n\pi}{N\tau}[(m-m')\tau-a\tau]}\right|^2 da \\
&= \tau\sum_{m'=1}^{N}\int_0^1\left|\frac{e^{i\frac{2n\pi}{N}(m'+a-1)} - e^{-i\frac{2n\pi}{N}}e^{i\frac{2n\pi}{N}a}}{1-e^{-i\frac{2n\pi}{N}}} + \frac{e^{i\frac{2n\pi}{N}(1-a)} - e^{i\frac{2n\pi}{N}}e^{i\frac{2n\pi}{N}(N-m'-a)}}{1-e^{i\frac{2n\pi}{N}}}\right|^2 da \\
&= \tau\sum_{m'=1}^{N}\int_0^1\left|\frac{e^{i\frac{2n\pi}{N}(m'+a-1)} - e^{i\frac{2n\pi}{N}(a-1)}}{1-e^{-i\frac{2n\pi}{N}}} - \frac{e^{-i\frac{2n\pi}{N}a} - e^{i\frac{2n\pi}{N}(N-m'-a)}}{1-e^{-i\frac{2n\pi}{N}}}\right|^2 da \\
&= \tau\left|\frac{1}{1-e^{-i\frac{2n\pi}{N}}}\right|^2\sum_{m'=1}^{N}\int_0^1\left|e^{i\frac{2n\pi}{N}(a-1)}\left(e^{i\frac{2n\pi}{N}m'}-1\right) + e^{-i\frac{2n\pi}{N}a}\left(e^{-i\frac{2n\pi}{N}m'}-1\right)\right|^2 da \\
&= \tau\left|\frac{1}{1-e^{-i\frac{2n\pi}{N}}}\right|^2\sum_{m'=1}^{N}\int_{-1/2}^{1/2}\left|e^{i\frac{2n\pi}{N}(a-1/2)}\left(e^{i\frac{2n\pi}{N}m'}-1\right) + e^{-i\frac{2n\pi}{N}(a+1/2)}\left(e^{-i\frac{2n\pi}{N}m'}-1\right)\right|^2 da \\
&= \tau\left|\frac{1}{1-e^{-i\frac{2n\pi}{N}}}\right|^2\sum_{m'=1}^{N}\int_{-1/2}^{1/2}\left|e^{i\frac{2n\pi}{N}a}\left(e^{i\frac{2n\pi}{N}m'}-1\right) + e^{-i\frac{2n\pi}{N}a}\left(e^{-i\frac{2n\pi}{N}m'}-1\right)\right|^2 da
\end{aligned}
$$

$$
\begin{aligned}
&= \tau \left| \frac{2}{1-e^{-i\frac{2n\pi}{N}}} \right|^2 \sum_{m'=1}^{N} \int_{-1/2}^{1/2} \left| \cos\left(\frac{2n\pi}{N}[m'+a]\right) - \cos\left(\frac{2n\pi}{N}a\right) \right|^2 da \\
&= \tau \left| \frac{4}{1-e^{-i\frac{2n\pi}{N}}} \right|^2 \sum_{m'=1}^{N} \left| \sin\left(\frac{n\pi}{N}m'\right) \right|^2 \int_{-1/2}^{1/2} \left| \sin\left(\frac{n\pi}{N}[m'+2a]\right) \right|^2 da \\
&= \tau \frac{1}{2} \left| \frac{4}{1-e^{-i\frac{2n\pi}{N}}} \right|^2 \sum_{m'=1}^{N} \left| \sin\left(\frac{n\pi}{N}m'\right) \right|^2 \int_{-1/2}^{1/2} \left[1 - \cos\left(\frac{2n\pi}{N}[m'+2a]\right) \right] da \\
&= \tau \frac{1}{2} \left| \frac{4}{1-e^{-i\frac{2n\pi}{N}}} \right|^2 \sum_{m'=1}^{N} \sin^2\left(\frac{n\pi}{N}m'\right) \left[1 - \frac{N}{4n\pi} \left(\sin\left[\frac{2n\pi}{N}(m'+1)\right] - \sin\left[\frac{2n\pi}{N}(m'-1)\right] \right) \right] \\
&= \tau \frac{1}{4} \left| \frac{4}{1-e^{-i\frac{2n\pi}{N}}} \right|^2 \sum_{m'=1}^{N} \left[1 - \cos\left(\frac{2n\pi}{N}m'\right) \right] \left[1 - \frac{N}{2n\pi} \cos\left(\frac{2n\pi}{N}m'\right) \sin\left(\frac{2n\pi}{N}\right) \right]. \qquad \text{(E3)}
\end{aligned}
$$

Using the identity $\sum_{m'=1}^{N} \cos\left(\frac{2n\pi}{N}m'\right) = 0$, we obtain

$$
\begin{aligned}
\int_0^{\mathcal{T}} \left| \sum_m e^{i\frac{2n\pi}{N\tau}|t'-\tau_m|} \right|^2 dt' &= \tau \frac{1}{4} \left| \frac{4}{1-e^{-i\frac{2n\pi}{N}}} \right|^2 \sum_{m'=1}^{N} \left[1 - \cos\left(\frac{2n\pi}{N}m'\right) \right] \left[1 - \frac{N}{2n\pi} \cos\left(\frac{2n\pi}{N}m'\right) \sin\left(\frac{2n\pi}{N}\right) \right] \\
&= \tau \frac{1}{4} \left| \frac{4}{1-e^{-i\frac{2n\pi}{N}}} \right|^2 \sum_{m'=1}^{N} \left[1 + \frac{N}{2n\pi} \cos^2\left(\frac{2n\pi}{N}m'\right) \sin\left(\frac{2n\pi}{N}\right) \right] \\
&= \tau \frac{1}{4} \left| \frac{4}{1-e^{-i\frac{2n\pi}{N}}} \right|^2 \sum_{m'=1}^{N} \left[1 + \frac{N}{4n\pi} \sin\left(\frac{2n\pi}{N}\right) + \frac{N}{4n\pi} \sin\left(\frac{2n\pi}{N}\right) \cos\left(\frac{4n\pi}{N}m'\right) \right] \\
&= \tau \left| \frac{1}{1-e^{-i\frac{2n\pi}{N}}} \right|^2 4N \left[1 + \frac{N}{4n\pi} \sin\left(\frac{2n\pi}{N}\right) \right] = \frac{N\tau}{\sin^2\left(\frac{n\pi}{N}\right)} \left[1 + \frac{N}{4n\pi} \sin\left(\frac{2n\pi}{N}\right) \right] \\
&= 2N\tau \frac{1 + \frac{N}{4n\pi} \sin\left(\frac{2n\pi}{N}\right)}{1 - \cos\left(\frac{2n\pi}{N}\right)}. \qquad \text{(E4)}
\end{aligned}
$$

Plugging the above result into Eq. (E2), we find the total field strength left in the waveguide:

$$
I(n) = \frac{2N\gamma\tau \, \sin^2\left(\frac{n\pi}{N}\right)}{\left[2 \, \sin^2\left(\frac{n\pi}{N} + N\gamma\tau\right)\right]^2} \left[1 + \frac{N}{4n\pi} \sin\left(\frac{2n\pi}{N}\right) \right]. \qquad \text{(E5)}
$$

APPENDIX F: TOTAL FIELD INTENSITY OF AN OSCILLATING BOUND STATE

The total field intensity of an oscillating bound state with two coexisting dark states s_{n_1} and s_{n_2} is

$$
\begin{aligned}
I(n_1, n_2) &= \frac{\gamma}{2} \int_0^{\mathcal{T}} \left| \sum_m A(n_1) e^{-i\frac{2n_1\pi}{N\tau}(t-|t'-\tau_m|)} + A(n_2) e^{-i\frac{2n_2\pi}{N\tau}(t-|t'-\tau_m|)} \right|^2 dt' \\
&= \frac{\gamma\tau}{2} \sum_{m'=1}^{N} \int_0^1 \left| A(n_1) e^{-i\frac{2n_1\pi}{N\tau}t} \left(\sum_{m=1}^{m'} e^{i\frac{2n_1\pi}{N\tau}[(m'-m)\tau + a\tau]} + \sum_{m=m'+1}^{N} e^{i\frac{2n_1\pi}{N\tau}[(m-m')\tau - a\tau]} \right) \right. \\
&\quad \left. + A(n_2) e^{-i\frac{2n_2\pi}{N\tau}t} \left(\sum_{m=1}^{m'} e^{i\frac{2n_2\pi}{N\tau}[(m'-m)\tau + a\tau]} + \sum_{m=m'+1}^{N} e^{i\frac{2n_2\pi}{N\tau}[(m-m')\tau - a\tau]} \right) \right|^2 da \\
&= \frac{\gamma\tau}{2} \sum_{m'=1}^{N} \int_0^1 \left| A(n_1) e^{-i\frac{2n_1\pi}{N\tau}t} \left(\frac{e^{i\frac{2n_1\pi}{N}(m'+a-1)} - e^{i\frac{2n_1\pi}{N}(a-1)}}{1 - e^{-i\frac{2n_1\pi}{N}}} - \frac{e^{-i\frac{2n_1\pi}{N}a} - e^{i\frac{2n_1\pi}{N}(N-m'-a)}}{1 - e^{-i\frac{2n_1\pi}{N}}} \right) \right. \\
&\quad \left. + A(n_2) e^{-i\frac{2n_2\pi}{N\tau}t} \left(\frac{e^{i\frac{2n_2\pi}{N}(m'+a-1)} - e^{i\frac{2n_2\pi}{N}(a-1)}}{1 - e^{-i\frac{2n_2\pi}{N}}} - \frac{e^{-i\frac{2n_2\pi}{N}a} - e^{i\frac{2n_2\pi}{N}(N-m'-a)}}{1 - e^{-i\frac{2n_2\pi}{N}}} \right) \right|^2 da
\end{aligned}
$$

$$
\begin{aligned}
&= \frac{\gamma\tau}{2}\sum_{m'=1}^{N}\int_0^1 \left| \frac{A(n_1)e^{-i\frac{2n_1\pi}{N\tau}t}}{1-e^{-i\frac{2n_1\pi}{N}}}\left[e^{i\frac{2n_1\pi}{N}(a-1)}\left(e^{i\frac{2n_1\pi}{N}m'}-1\right)+e^{-i\frac{2n_1\pi}{N}a}\left(e^{-i\frac{2n_1\pi}{N}m'}-1\right)\right]\right.\\
&\quad \left. + \frac{A(n_2)e^{-i\frac{2n_2\pi}{N\tau}t}}{1-e^{-i\frac{2n_2\pi}{N}}}\left[e^{i\frac{2n_2\pi}{N}(a-1)}\left(e^{i\frac{2n_2\pi}{N}m'}-1\right)+e^{-i\frac{2n_2\pi}{N}a}\left(e^{-i\frac{2n_2\pi}{N}m'}-1\right)\right]\right|^2 da\\
&= \frac{\gamma\tau}{2}\sum_{m'=1}^{N}\int_{-1/2}^{1/2} \left| \frac{A(n_1)e^{-i\frac{2n_1\pi}{N\tau}\left(t+\frac{\tau}{2}\right)}}{1-e^{-i\frac{2n_1\pi}{N}}}\left[e^{i\frac{2n_1\pi}{N}a}\left(e^{i\frac{2n_1\pi}{N}m'}-1\right)+e^{-i\frac{2n_1\pi}{N}a}\left(e^{-i\frac{2n_1\pi}{N}m'}-1\right)\right]\right.\\
&\quad \left. + \frac{A(n_2)e^{-i\frac{2n_2\pi}{N\tau}\left(t+\frac{\tau}{2}\right)}}{1-e^{-i\frac{2n_2\pi}{N}}}\left[e^{i\frac{2n_2\pi}{N}a}\left(e^{i\frac{2n_2\pi}{N}m'}-1\right)+e^{-i\frac{2n_2\pi}{N}a}\left(e^{-i\frac{2n_2\pi}{N}m'}-1\right)\right]\right|^2 da\\
&= \frac{\gamma\tau}{2}\sum_{m'=1}^{N}\int_{-1/2}^{1/2} \left| \frac{2A(n_1)e^{-i\frac{2n_1\pi}{N\tau}\left(t+\frac{\tau}{2}\right)}}{1-e^{-i\frac{2n_1\pi}{N}}}\left[\cos\left(\frac{2n_1\pi}{N}[m'+a]\right)-\cos\left(\frac{2n_1\pi}{N}a\right)\right]\right.\\
&\quad \left. + \frac{2A(n_2)e^{-i\frac{2n_2\pi}{N\tau}\left(t+\frac{\tau}{2}\right)}}{1-e^{-i\frac{2n_2\pi}{N}}}\left[\cos\left(\frac{2n_2\pi}{N}[m'+a]\right)-\cos\left(\frac{2n_2\pi}{N}a\right)\right]\right|^2 da\\
&= \frac{\gamma\tau}{2}\sum_{m'=1}^{N}\int_{-1/2}^{1/2} \left| \frac{4A(n_1)e^{-i\frac{2n_1\pi}{N\tau}\left(t+\frac{\tau}{2}\right)}}{1-e^{-i\frac{2n_1\pi}{N}}}\sin\left(\frac{n_1\pi}{N}m'\right)\sin\left(\frac{n_1\pi}{N}[m'+2a]\right)\right.\\
&\quad \left. + \frac{4A(n_2)e^{-i\frac{2n_2\pi}{N\tau}\left(t+\frac{\tau}{2}\right)}}{1-e^{-i\frac{2n_2\pi}{N}}}\sin\left(\frac{n_2\pi}{N}m'\right)\sin\left(\frac{n_2\pi}{N}[m'+2a]\right)\right|^2 da\\
&= I(n_1)+I(n_2)+\frac{\gamma\tau}{2}16A(n_1)A(n_2)\left[\frac{e^{-i\frac{2(n_1-n_2)\pi}{N\tau}\left(t+\frac{\tau}{2}\right)}}{\left(1-e^{-i\frac{2n_1\pi}{N}}\right)\left(1-e^{i\frac{2n_2\pi}{N}}\right)}+\text{H.c.}\right]\\
&\quad \times\sum_{m'=1}^{N}\sin\left(\frac{n_1\pi}{N}m'\right)\sin\left(\frac{n_2\pi}{N}m'\right)\int_{-1/2}^{1/2}\sin\left(\frac{n_1\pi}{N}[m'+2a]\right)\sin\left(\frac{n_2\pi}{N}[m'+2a]\right)da\\
&= I(n_1)+I(n_2)+\frac{\gamma\tau}{2}16A(n_1)A(n_2)\left[\frac{e^{-i\frac{2(n_1-n_2)\pi}{N\tau}t}}{4\sin\left(\frac{n_1\pi}{N}\right)\sin\left(\frac{n_2\pi}{N}\right)}+\text{H.c.}\right]\\
&\quad \times\frac{1}{2}\sum_{m'=1}^{N}\sin\left(\frac{n_1\pi}{N}m'\right)\sin\left(\frac{n_2\pi}{N}m'\right)\int_{-1/2}^{1/2}\left[\cos\left(\frac{[n_1-n_2]\pi}{N}[m'+2a]\right)-\cos\left(\frac{[n_1+n_2]\pi}{N}[m'+2a]\right)\right]da\\
&= I(n_1)+I(n_2)+2\gamma\tau\frac{A(n_1)A(n_2)}{\sin\left(\frac{n_1\pi}{N}\right)\sin\left(\frac{n_2\pi}{N}\right)}\cos\left(\frac{2[n_1-n_2]\pi}{N\tau}t\right)\\
&\quad \times\sum_{m'=1}^{N}\sin\left(\frac{n_1\pi}{N}m'\right)\sin\left(\frac{n_2\pi}{N}m'\right)\int_{-1/2}^{1/2}\left[\cos\left(\frac{[n_1-n_2]\pi}{N}[m'+2a]\right)-\cos\left(\frac{[n_1+n_2]\pi}{N}[m'+2a]\right)\right]da\\
&= I(n_1)+I(n_2)+2\gamma\tau\frac{A(n_1)A(n_2)}{\sin\left(\frac{n_1\pi}{N}\right)\sin\left(\frac{n_2\pi}{N}\right)}\cos\left(\frac{2[n_1-n_2]\pi}{N\tau}t\right)\\
&\quad \times\sum_{m'=1}^{N}\sin\left(\frac{n_1\pi}{N}m'\right)\sin\left(\frac{n_2\pi}{N}m'\right)\left[\frac{N}{(n_1-n_2)\pi}\sin\left(\frac{[n_1-n_2]\pi}{N}\right)\cos\left(\frac{[n_1-n_2]\pi}{N}m'\right)\right.\\
&\quad \left. -\frac{N}{(n_1+n_2)\pi}\sin\left(\frac{[n_1+n_2]\pi}{N}\right)\cos\left(\frac{[n_1+n_2]\pi}{N}m'\right)\right]\\
&= I(n_1)+I(n_2)+2\gamma\tau\frac{A(n_1)A(n_2)}{\sin\left(\frac{n_1\pi}{N}\right)\sin\left(\frac{n_2\pi}{N}\right)}\cos\left(\frac{2[n_1-n_2]\pi}{N\tau}t\right)\\
&\quad \times\frac{1}{2}\sum_{m'=1}^{N}\left[\cos\left(\frac{[n_1-n_2]\pi}{N}m'\right)-\cos\left(\frac{[n_1+n_2]\pi}{N}m'\right)\right]
\end{aligned}
$$

$$\times\left[\frac{N}{(n_1-n_2)\pi}\sin\left(\frac{[n_1-n_2]\pi}{N}\right)\cos\left(\frac{[n_1-n_2]\pi}{N}m'\right)-\frac{N}{(n_1+n_2)\pi}\sin\left(\frac{[n_1+n_2]\pi}{N}\right)\cos\left(\frac{[n_1+n_2]\pi}{N}m'\right)\right]$$
$$=I(n_1)+I(n_2)+2N\gamma\tau\frac{A(n_1)A(n_2)}{4\sin\left(\frac{n_1\pi}{N}\right)\sin\left(\frac{n_2\pi}{N}\right)}\left[\frac{N}{(n_1-n_2)\pi}\sin\left(\frac{[n_1-n_2]\pi}{N}\right)+\frac{N}{(n_1+n_2)\pi}\sin\left(\frac{[n_1+n_2]\pi}{N}\right)\right]$$
$$\times\cos\left(\frac{2[n_1-n_2]\pi}{N\tau}t\right). \tag{F1}$$

Here, $I(n)$ is defined by Eq. (E5). Using the condition in Eq. (12) in the main text, we finally obtain

$$I(n_1,n_2)=I(n_1)+I(n_2)-2A(n_1)A(n_2)\left[1+\frac{(n_1-n_2)\sin\left(\frac{n_1+n_2}{N}\pi\right)}{(n_1+n_2)\sin\left(\frac{n_1-n_2}{N}\pi\right)}\right]\cos\left(\frac{2[n_1-n_2]\pi}{N\tau}t\right). \tag{F2}$$

For the two dark modes $\Omega_{n_1}=2n_1\pi/(N\tau)$ and $\Omega_{n_2}=2n_2\pi/(N\tau)$, we have

$$\begin{aligned}\Omega_{n_1}+\Omega_{n_2}&=\frac{2(n_1+n_2)\pi}{N\tau}\\&=\Omega\frac{2(n_1+n_2)\pi}{2n_1\pi-2(n_1-n_2)\pi\frac{\cot\left(\frac{n_1\pi}{N}\right)}{\cot\left(\frac{n_1\pi}{N}\right)-\cot\left(\frac{n_2\pi}{N}\right)}}\\&=\Omega\frac{2(n_1+n_2)\pi}{2n_1\pi+2(n_1-n_2)\pi\frac{\cos\left(\frac{n_1\pi}{N}\right)\sin\left(\frac{n_2\pi}{N}\right)}{\sin\left(\frac{[n_1-n_2]\pi}{N}\right)}}\\&=\Omega\frac{2(n_1+n_2)\pi}{2n_1\pi+(n_1-n_2)\pi\frac{\sin\left(\frac{[n_1+n_2]\pi}{N}\right)-\sin\left(\frac{[n_1-n_2]\pi}{N}\right)}{\sin\left(\frac{[n_1-n_2]\pi}{N}\right)}}\\&=\Omega\frac{2(n_1+n_2)\pi}{(n_1+n_1)\pi+(n_1-n_2)\pi\frac{\sin\left(\frac{[n_1+n_2]\pi}{N}\right)}{\sin\left(\frac{[n_1-n_2]\pi}{N}\right)}}\\&=\frac{2\Omega}{1+\frac{(n_1-n_2)\sin\left(\frac{n_1+n_2}{N}\pi\right)}{(n_1+n_2)\sin\left(\frac{n_1-n_2}{N}\pi\right)}}.\end{aligned} \tag{F3}$$

In the second step, we again used the condition in Eq. (12) in the main text. The final result is

$$I(n_1,n_2)=I(n_1)+I(n_2)-4A(n_1)A(n_2)\frac{\Omega}{\Omega_{n_1}+\Omega_{n_2}}\cos\left([\Omega_{n_1}-\Omega_{n_2}]t\right), \tag{F4}$$

which is exactly Eq. (15) in the main text.

[1] A. F. Kockum, A. Miranowicz, S. De Liberato, S. Savasta, and F. Nori, Ultrastrong coupling between light and matter, Nat. Rev. Phys. **1**, 19 (2019).

[2] P. Goy, J. M. Raimond, M. Gross, and S. Haroche, Observation of Cavity-Enhanced Single-Atom Spontaneous Emission, Phys. Rev. Lett. **50**, 1903 (1983).

[3] D. Leibfried, R. Blatt, C. Monroe, and D. Wineland, Quantum dynamics of single trapped ions, Rev. Mod. Phys. **75**, 281 (2003).

[4] A. Wallraff, D. I. Schuster, A. Blais, L. Frunzio, R.-S. Huang, J. Majer, S. Kumar, S. M. Girvin, and R. J. Schoelkopf, Strong coupling of a single photon to a superconducting qubit using circuit quantum electrodynamics, Nature (London) **431**, 162 (2004).

[5] R. Miller, T. E. Northup, K. M. Birnbaum, A. Boca, A. D. Boozer, and H. J. Kimble, Trapped atoms in cavity QED: coupling quantized light and matter, J. Phys. B: At., Mol. Opt. Phys. **38**, S551 (2005).

[6] S. Haroche, Nobel Lecture: Controlling photons in a box and exploring the quantum to classical boundary, Rev. Mod. Phys. **85**, 1083 (2013).

[7] X. Gu, A. F. Kockum, A. Miranowicz, Y.-X. Liu, and F. Nori, Microwave photonics with superconducting quantum circuits, Phys. Rep. **718–719**, 1 (2017).

[8] D. F. Walls and G. J. Milburn, *Quantum Optics*, 2nd ed. (Springer, Berlin, 2008).

[9] J. Q. You and F. Nori, Atomic physics and quantum optics using superconducting circuits, Nature (London) **474**, 589 (2011).

[10] A. F. Kockum and F. Nori, Quantum Bits with Josephson Junctions, in *Fundamentals and Frontiers of the Josephson Effect*, edited by F. Tafuri (Springer, Berlin, 2019), pp. 703–741.

[11] P. Krantz, M. Kjaergaard, F. Yan, T. P. Orlando, S. Gustavsson, and W. D. Oliver, A quantum engineer's guide to superconducting qubits, Appl. Phys. Rev. **6**, 021318 (2019).

[12] A. F. Kockum, Quantum optics with giant atoms - the first five years, arXiv:1912.13012.

[13] J. Koch, T. M. Yu, J. Gambetta, A. A. Houck, D. I. Schuster, J. Majer, A. Blais, M. H. Devoret, S. M. Girvin, and R. J. Schoelkopf, Charge-insensitive qubit design derived from the Cooper pair box, Phys. Rev. A **76**, 042319 (2007).

[14] M. V. Gustafsson, T. Aref, A. F. Kockum, M. K. Ekström, G. Johansson, and P. Delsing, Propagating phonons coupled to an artificial atom, Science **346**, 207 (2014).

[15] T. Aref, P. Delsing, M. K. Ekström, A. F. Kockum, M. V. Gustafsson, G. Johansson, P. J. Leek, E. Magnusson, and R. Manenti, Quantum acoustics with surface acoustic waves, in *Superconducting Devices in Quantum Optics*, edited by R. H. Hadfield and G. Johansson (Springer, Berlin, 2016).

[16] G. Andersson, B. Suri, L. Guo, T. Aref, and P. Delsing, Non-exponential decay of a giant artificial atom, Nat. Phys. **15**, 1123 (2019).

[17] R. Manenti, A. F. Kockum, A. Patterson, T. Behrle, J. Rahamim, G. Tancredi, F. Nori, and P. J. Leek, Circuit quantum acoustodynamics with surface acoustic waves, Nat. Commun. **8**, 975 (2017).

[18] A. Noguchi, R. Yamazaki, Y. Tabuchi, and Y. Nakamura, Qubit-Assisted Transduction for a Detection of Surface Acoustic Waves near the Quantum Limit, Phys. Rev. Lett. **119**, 180505 (2017).

[19] B. A. Moores, L. R. Sletten, J. J. Viennot, and K. W. Lehnert, Cavity Quantum Acoustic Device in the Multimode Strong Coupling Regime, Phys. Rev. Lett. **120**, 227701 (2018).

[20] K. J. Satzinger, Y. P. Zhong, H.-S. Chang, G. A. Peairs, A. Bienfait, M.-H. Chou, A. Y. Cleland, C. R. Conner, É. Dumur, J. Grebel, I. Gutierrez, B. H. November, R. G. Povey, S. J. Whiteley, D. D. Awschalom, D. I. Schuster, and A. N. Cleland, Quantum control of surface acoustic-wave phonons, Nature (London) **563**, 661 (2018).

[21] A. N. Bolgar, J. I. Zotova, D. D. Kirichenko, I. S. Besedin, A. V. Semenov, R. S. Shaikhaidarov, and O. V. Astafiev, Quantum Regime of a Two-Dimensional Phonon Cavity, Phys. Rev. Lett. **120**, 223603 (2017).

[22] L. R. Sletten, B. A. Moores, J. J. Viennot, and K. W. Lehnert, Resolving Phonon Fock States in a Multimode Cavity with a Double-Slit Qubit, Phys. Rev. X **9**, 021056 (2019).

[23] A. Bienfait, K. J. Satzinger, Y. P. Zhong, H.-S. Chang, M.-H. Chou, C. R. Conner, É. Dumur, J. Grebel, G. A. Peairs, R. G. Povey, and A. N. Cleland, Phonon-mediated quantum state transfer and remote qubit entanglement, Science **364**, 368 (2019).

[24] R. Barends, J. Kelly, A. Megrant, D. Sank, E. Jeffrey, Y. Chen, Y. Yin, B. Chiaro, J. Mutus, C. Neill, P. O'Malley, P. Roushan, J. Wenner, T. C. White, A. N. Cleland, and J. M. Martinis, Coherent Josephson Qubit Suitable for Scalable Quantum Integrated Circuits, Phys. Rev. Lett. **111**, 080502 (2013).

[25] A. F. Kockum, P. Delsing, and G. Johansson, Designing frequency-dependent relaxation rates and Lamb shifts for a giant artificial atom, Phys. Rev. A **90**, 013837 (2014).

[26] B. Kannan, M. Ruckriegel, D. Campbell, A. F. Kockum, J. Braumüller, D. Kim, M. Kjaergaard, P. Krantz, A. Melville, B. M. Niedzielski, A. Vepsäläinen, R. Winik, J. Yoder, F. Nori, T. P. Orlando, S. Gustavsson, and W. D. Oliver, Waveguide quantum electrodynamics with superconducting artificial giant atoms, Nature (London) **583**, 775 (2020).

[27] A. M. Vadiraj, A. Ask, T. G. McConkey, I. Nsanzineza, C. W. Sandbo Chang, A. F. Kockum, and C. M. Wilson, Engineering the level structure of a giant artificial atom in waveguide quantum electrodynamics, arXiv:2003.14167.

[28] A. F. Kockum, G. Johansson, and F. Nori, Decoherence-Free Interaction between Giant Atoms in Waveguide Quantum Electrodynamics, Phys. Rev. Lett. **120**, 140404 (2018).

[29] A. González-Tudela, C. Sánchez Muñoz, and J. I. Cirac, Engineering and Harnessing Giant Atoms in High-Dimensional Baths: A Proposal for Implementation with Cold Atoms, Phys. Rev. Lett. **122**, 203603 (2019).

[30] J. Eschner, C. Raab, F. Schmidt-Kaler, and R. Blatt, Light interference from single atoms and their mirror images, Nature (London) **413**, 495 (2001).

[31] U. Dorner and P. Zoller, Laser-driven atoms in half-cavities, Phys. Rev. A **66**, 023816 (2002).

[32] T. Tufarelli, M. S. Kim, and F. Ciccarello, Non-Markovianity of a quantum emitter in front of a mirror, Phys. Rev. A **90**, 012113 (2014).

[33] P.-O. Guimond, M. Pletyukhov, H. Pichler, and P. Zoller, Delayed coherent quantum feedback from a scattering theory and a matrix product state perspective, Quantum Sci. Technol. **2**, 044012 (2017).

[34] G. Calajó, Y.-L. L. Fang, H. U. Baranger, and F. Ciccarello, Exciting a Bound State in the Continuum through Multiphoton Scattering Plus Delayed Quantum Feedback, Phys. Rev. Lett. **122**, 073601 (2019).

[35] P. W. Milonni and P. L. Knight, Retardation in the resonant interaction of two identical atoms, Phys. Rev. A **10**, 1096 (1974).

[36] H. Zheng and H. U. Baranger, Persistent Quantum Beats and Long-Distance Entanglement from Waveguide-Mediated Interactions, Phys. Rev. Lett. **110**, 113601 (2013).

[37] C. Gonzalez-Ballestero, F. J. Garcia-Vidal, and E. Moreno, Non-Markovian effects in waveguide-mediated entanglement, New J. Phys. **15**, 073015 (2013).

[38] M. Laakso and M. Pletyukhov, Scattering of Two Photons from Two Distant Qubits: Exact Solution, Phys. Rev. Lett. **113**, 183601 (2014).

[39] C. Gonzalez-Ballestero, E. Moreno, and F. J. Garcia-Vidal, Generation, manipulation, and detection of two-qubit entanglement in waveguide QED, Phys. Rev. A **89**, 042328 (2014).

[40] Y.-L. L. Fang and H. U. Baranger, Waveguide QED: Power spectra and correlations of two photons scattered off multiple distant qubits and a mirror, Phys. Rev. A **91**, 053845 (2015).

[41] P.-O. Guimond, A. Roulet, H. N. Le, and V. Scarani, Rabi oscillation in a quantum cavity: Markovian and non-Markovian dynamics, Phys. Rev. A **93**, 023808 (2016).

[42] T. Ramos, B. Vermersch, P. Hauke, H. Pichler, and P. Zoller, Non-Markovian dynamics in chiral quantum networks with spins and photons, Phys. Rev. A **93**, 062104 (2016).

[43] F. Dinc, I. Ercan, and A. M. Branczyk, Exact Markovian and non-Markovian time dynamics in waveguide QED: collective interactions, bound states in continuum, superradiance and subradiance, Quantum **3**, 213 (2019).

[44] H.-P. Breuer, E.-M. Laine, J. Piilo, and B. Vacchini, Colloquium: Non-Markovian dynamics in open quantum systems, Rev. Mod. Phys. **88**, 021002 (2016).

[45] S. Rist, J. Eschner, M. Hennrich, and G. Morigi, Photon-mediated interaction between two distant atoms, Phys. Rev. A **78**, 013808 (2008).

[46] D. Gribben, A. Strathearn, J. Iles-Smith, D. Kilda, A. Nazir, B. W. Lovett, and P. Kirton, Exact quantum dynamics in structured environments, Phys. Rev. Res. **2**, 013265 (2020).

[47] Q.-J. Tong, J.-H. An, H.-G. Luo, and C. H. Oh, Mechanism of entanglement preservation, Phys. Rev. A **81**, 052330 (2010).

[48] S. Garmon, T. Petrosky, L. Simine, and D. Segal, Amplification of non-Markovian decay due to bound state absorption into continuum, Fortschr. Phys. **61**, 261 (2013).

[49] Y. Wang, M. J. Gullans, A. Browaeys, J. V. Porto, D. E. Chang, and A. V. Gorshkov, Single-photon bound states in atomic ensembles, arXiv:1809.01147.

[50] P. Facchi, M. S. Kim, S. Pascazio, F. V. Pepe, D. Pomarico, and T. Tufarelli, Bound states and entanglement generation in waveguide quantum electrodynamics, Phys. Rev. A **94**, 043839 (2016).

[51] G. Calajó, F. Ciccarello, D. Chang, and P. Rabl, Atom-field dressed states in slow-light waveguide QED, Phys. Rev. A **93**, 033833 (2016).

[52] T. Shi, Y.-H. Wu, A. González-Tudela, and J. I. Cirac, Bound States in Boson Impurity Models, Phys. Rev. X **6**, 021027 (2016).

[53] A. González-Tudela and J. I. Cirac, Quantum Emitters in Two-Dimensional Structured Reservoirs in the Nonperturbative Regime, Phys. Rev. Lett. **119**, 143602 (2017).

[54] A. González-Tudela and J. I. Cirac, Markovian and non-Markovian dynamics of quantum emitters coupled to two-dimensional structured reservoirs, Phys. Rev. A **96**, 043811 (2017).

[55] Y. Liu and A. A. Houck, Quantum electrodynamics near a photonic bandgap, Nat. Phys. **13**, 48 (2017).

[56] N. M. Sundaresan, R. Lundgren, G. Zhu, A. V. Gorshkov, and A. A. Houck, Interacting Qubit-Photon Bound States with Superconducting Circuits, Phys. Rev. X **9**, 011021 (2019).

[57] E. Cortese, I. Carusotto, R. Colombelli, and S. De Liberato, Strong coupling of ionizing transitions, Optica **6**, 354 (2019).

[58] L. Qiao, Y.-J. Song, and C.-P. Sun, Quantum phase transition and interference trapping of populations in a coupled-resonator waveguide, Phys. Rev. A **100**, 013825 (2019).

[59] Wei Zhao and Zhihai Wang, Single-photon scattering and bound states in an atom-waveguide system with two or multiple coupling points, Phys. Rev. A **101**, 053855 (2020).

[60] Xin Wang, T. Liu, A. F. Kockum, H.-R. Li, and F. Nori, Tunable chiral bound states with giant atoms, arXiv:2008.13560.

[61] J. S. Douglas, H. Habibian, C.-L. Hung, A. V. Gorshkov, H. J. Kimble, and D. E. Chang, Quantum many-body models with cold atoms coupled to photonic crystals, Nat. Photonics **9**, 326 (2015).

[62] A. González-Tudela and J. I. Cirac, Exotic quantum dynamics and purely long-range coherent interactions in Dirac conelike baths, Phys. Rev. A **97**, 043831 (2018).

[63] L. Guo, A. L. Grimsmo, A. F. Kockum, M. Pletyukhov, and G. Johansson, Giant acoustic atom: A single quantum system with a deterministic time delay, Phys. Rev. A **95**, 053821 (2017).

[64] A. Ask, M. Ekström, P. Delsing, and G. Johansson, Cavity-free vacuum-Rabi splitting in circuit quantum acoustodynamics, Phys. Rev. A **99**, 013840 (2019).

[65] See Supplemental Material Video at http://link.aps.org/supplemental/10.1103/PhysRevResearch.2.043014 for an animation of the time evolution of the atomic and waveguide occupation probabilities for the oscillating bound state shown in Fig. 3(b).

[66] W. D. Oliver and P. B. Welander, Materials in superconducting quantum bits, MRS Bull. **38**, 816 (2013).

[67] J. J. Burnett, A. Bengtsson, M. Scigliuzzo, D. Niepce, M. Kudra, P. Delsing, and J. Bylander, Decoherence benchmarking of superconducting qubits, npj Quantum Inf. **5**, 54 (2019).

[68] M. Kjaergaard, M. E. Schwartz, J. Braumüller, P. Krantz, J. I.-J. Wang, S. Gustavsson, and W. D. Oliver, Superconducting Qubits: Current State of Play, Annu. Rev. Condens. Matter Phys. **11**, 369 (2020).

[69] L. Guo *et al.* (unpublished).

[70] M. Mirhosseini, E. Kim, X. Zhang, A. Sipahigil, P. B. Dieterle, A. J. Keller, A. Asenjo-Garcia, D. E. Chang, and O. Painter, Cavity quantum electrodynamics with atom-like mirrors, Nature (London) **569**, 692 (2019).

[71] B. Peropadre, J. Lindkvist, I.-C. Hoi, C. M. Wilson, J. J. Garcia-Ripoll, P. Delsing, and G. Johansson, Scattering of coherent states on a single artificial atom, New J. Phys. **15**, 035009 (2013).

[72] M. O. Scully and M. S. Zubairy, *Quantum Optics* (Cambridge University Press, Cambridge, 1997).